

The pulsating variable star population in DDO210

Antonio J. Ordoñez^{1*} and Ata Sarajedini¹

¹*Department of Astronomy, University of Florida, 211 Bryant Space Science Center, Gainesville, FL 32611, USA*

Accepted 2015 October 23. Received 2015 October 20; in original form 2015 August 28

ABSTRACT

We have probed the pulsating variable star content of the isolated Local Group dwarf galaxy, DDO210 (Aquarius), using archival Advanced Camera for Surveys/*Hubble Space Telescope* imaging in the F475W and F814W passbands. We find a total of 32 RR Lyrae stars (24 ab-type; 8 c-type) and 75 Cepheid variables. The mean periods of the ab-type and c-type RR Lyrae stars are calculated to be $\langle P_{\text{ab}} \rangle = 0.609 \pm 0.011$ and $\langle P_{\text{c}} \rangle = 0.359 \pm 0.025$ days, respectively. The light curve properties of the fundamental mode RR Lyrae stars yield a mean metallicity of $\langle [\text{Fe}/\text{H}] \rangle = -1.63 \pm 0.11$ dex for this ancient population, consistent with a recent synthetic colour-magnitude diagram analysis. We find this galaxy to be Oosterhoff-intermediate and lacking in high-amplitude, short-period ab-type RR Lyrae, consistent with behavior recently observed for many dwarf spheroidals and ultra-faint dwarfs in the Local Group. We find a distance modulus of $\mu = 25.07 \pm 0.12$ as determined by the RR Lyrae stars, slightly larger but agreeing with recent distance estimates from the red giant branch tip. We also find a sizable population of Cepheid variables in this galaxy. We provide evidence in favor of most if not all of these stars being short-period classical Cepheids. Assuming all of these stars to be classical Cepheids, we find that most of these Cepheids are ~ 300 Myr old, with the youngest Cepheids being offset from the older Cepheids and the centre of the galaxy. We conclude that this may have resulted from a migration of star formation in DDO210.

Key words: galaxies: Dwarf – galaxies: individual: DDO210 – stars: abundances – stars: variables: RR Lyrae – stars: variables: Cepheids

1 INTRODUCTION

Dwarf galaxies are known to be the most numerous type of galaxy in general. Additionally, dwarf galaxy accretion has been proposed as one of the major mechanisms in the formation of massive galaxies, such as the Milky Way (MW) (Mateo 1998). While the notion of MW halo build-up from systems resembling modern day dwarf spheroidals (dSph) has encountered significant contention recently from element abundance ratio comparisons with the Galaxy (Venn et al. 2004; Pritzl, Venn, Irwin 2005) and the Oosterhoff dichotomy (Catelan 2009), accretion of dwarfs has certainly occurred, with the Sagittarius dSph providing a smoking gun for such interactions (Ibata, Gilmore, & Irwin 1994). Studying the stellar populations of Local Group (LG) dwarfs, especially the old ones, allows us to better constrain the extent to which these dwarfs have contributed to the Galactic halo. Dwarf galaxies also present unique astrophysical laboratories to study how these relatively simple galaxies have evolved

in different environments through their chemical enrichment and star formation histories (SFHs).

Variable stars are important tracers of the histories of dwarf galaxies. They provide unique insights into their parental stellar populations through the study of their light curves. Cepheid and RR Lyrae variables are especially useful in this context. For instance, classical Cepheids (CCs) are massive, blue-loop stars that are relatively young, having formed within the past ~ 1 Gyr (Bono et al. 2005). Therefore these stars trace young star formation events. On the other hand, RR Lyrae stars are ancient horizontal branch (HB) stars originating from low-mass stars, and thus trace star formation at ages ≥ 10 Gyr (see Figs. 2 and 3 of Lee, Demarque, & Zinn (1994) for theoretical modeling of RR Lyrae stars on the HB and Glatt et al. (2008) for an age determination of the youngest known system harboring RR Lyrae stars). Anomalous Cepheids (ACs) are thought to represent more intermediate-mass stars at low metallicities. They may trace intermediate age (1-6 Gyr) populations or old binary systems (Fiorentino & Monelli 2012). The mere presence of any combination of these stars thus provides constraints on the SFH of the host system.

* E-mail: a.ordonez@ufl.edu

In addition to informing the SFH of a stellar population, pulsating variables also provide insight into the chemical enrichment of such a population. Most notably, there are strong correlations between the light curve shapes of fundamental mode RR Lyrae, referred to in the literature as RRab stars, and their iron abundances, [Fe/H] (Jurcsik & Kovács 1996; Alcock et al. 2000; Nemeč et al. 2013). Similar relationships for Cepheids have recently been explored (Szabados et al. 2012; Klagyivik et al. 2013). Therefore, these stars provide a means to elucidate portions of the chemical enrichment history of a stellar population without the need for spectroscopic observations.

The LG dSph/Irr transition-type (dTrans; see Mateo (1998)) galaxy, DDO210 (Aquarius), is one of the most distant dwarf galaxies in the LG. While distance estimates to this galaxy have differed significantly over the past few decades, recent values have converged on a distance of $d \sim 1$ Mpc using the tip of the red giant branch (TRGB) (Cole et al. 2014). This galaxy is one of the most isolated in the LG and thus provides an excellent opportunity to study how such low-mass, isolated dwarfs evolve.

Recently, Cole et al. (2014) presented a synthetic colour-magnitude diagram (CMD) analysis of the SFH of DDO210 using their *Hubble Space Telescope* (*HST*)/Advanced Camera for Surveys (ACS) observations (GO-12925; PI: A. Cole). They find a complex SFH over the lifetime of DDO210 characterized by a long delay before the onset of a major star burst ~ 7 Gyr ago and followed by a relative lull in star formation for the past ~ 5 Gyr. The age-metallicity relation (AMR) produced by their analysis reveals very little chemical enrichment throughout its lifetime.

The goal of this work is to identify and characterize the pulsating variable stars within DDO210, thereby constraining its evolutionary history. In Section 2, we describe the data used for this study, and the reduction process performed on them. We detail the variable star identification and characterization processes in Section 3. We present the properties of the RR Lyrae and Cepheid stars in Sections 4 and 5 respectively. A discussion of the properties of these stars within the context of the SFH of DDO210 is given in Section 6, and the conclusions are presented in Section 7.

2 OBSERVATIONS AND DATA REDUCTION

The data set used by Cole et al. (2014) is very deep and covers a time baseline conducive to identifying short-period variable stars. These observations of DDO210 were originally intended for use in a detailed SFH analysis for this dwarf, and thus cover a significant portion of the galaxy while reaching photometric depths to the main-sequence turnoff. The observations consisting of 22,920 seconds in F475W and 33,480 seconds in F814W were taken with a cadence well-suited for identifying short-period variable stars. We retrieved these images from the Mikulski Archive for Space Telescopes (MAST)¹ for use in our study.

We downloaded the charge-transfer efficiency (CTE) corrected (**FLC*) images from MAST, which were also processed through the standard *HST* pipeline. Bad pixels

were then masked and the geometric correction pixel area maps were applied to each image. Photometry was then performed using the DAOPHOT/ALLSTAR/ALLFRAME software packages (Stetson 1987, 1994). Empirical point-spread functions (PSFs) were constructed using the brightest isolated stars in one cosmic-ray rejected reference image for each filter using the corresponding task in DAOPHOT. Aperture corrections were calculated from bright, isolated stars on each chip. The median aperture correction for these stars was then applied to all stars. We noticed a small photometric offset between the WFC1 and WFC2 chips after the aperture correction, and placed the WFC2 photometry on the same scale as the WFC1 photometry for consistency. The offsets amounted to 0.1 mag in F475W and -0.05 mag in F814W. We chose to correct WFC2 to the photometric system on WFC1 after comparison of our CMDs with that of Cole et al. (2014), who used the same data set, revealed that the WFC1 photometry agreed with theirs. We attribute this error to the lack of bright, isolated stars in the WFC2 field with which to obtain an accurate aperture correction value. Finally, conversion of the native *HST* VEGAMAG photometry to the ground-based Johnson-Cousins B and I filters was accomplished using the prescription from Sirianni et al. (2005).

3 VARIABLE STAR CHARACTERIZATION AND SIMULATIONS

3.1 Characterization

In order to identify potential variable stars within the photometry, we first applied cuts in magnitude and colour in order to narrow our region of interest. Since the primary goal of this work is to characterize the pulsating variable star content within the instability strip, we determined stars within $21 \text{ mag} < m_{\text{F814W}} < 27 \text{ mag}$ and $0 < m_{\text{F475W}} - m_{\text{F814W}} < 1.5 \text{ mag}$ to be an appropriate region of interest. Potential variables were identified using a reduced χ^2 defined as:

$$\chi^2 = \frac{1}{N_1 + N_2} \times \left[\sum_{i=1}^{N_1} \frac{(m_{1,i} - \bar{m}_1)^2}{\sigma_i^2} + \sum_{i=1}^{N_2} \frac{(m_{2,i} - \bar{m}_2)^2}{\sigma_i^2} \right] \quad (1)$$

In this case, m_1 and m_2 are the F475W and F814W magnitudes in the VEGAMAG photometric system. In an effort to filter spurious variables, we rejected $3\text{-}\sigma$ outliers from the χ^2 calculation for each light curve. Stars with $\chi^2 \geq 2$ were flagged as variable candidates.

The raw light curve of one of the variable candidates is shown in Fig. 1. This light curve illustrates the high quality of these data for identifying variable stars. Table 1 provides the full, time-series photometry for this star, and the photometry for all variable candidates is available in the online version of the journal.

Once we identified our set of variable candidates, we then removed data points from each light curve with anomalously high errors ($\gtrsim 0.1$ mag) to ensure a final sample of high fidelity light curves. Analysis of these light curves was then performed using template light curve fitting. This method, based largely off the technique originated by Layden et al. (1999), caters well to data sets with sparse or irregular time sampling and large gaps. We use RRFIT (Yang &

¹ <http://archive.stsci.edu/>

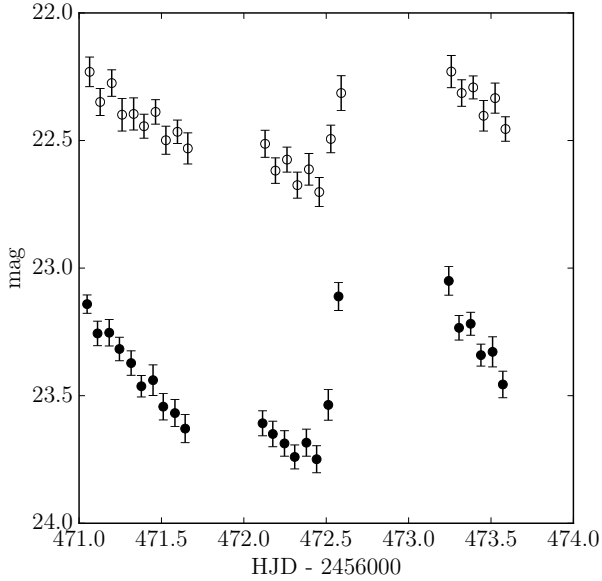


Figure 1. The raw, unphased light curve of one variable star candidate in our sample. The filled circles represent the F475W light curve, while the open circles are the F814W light curve data points.

Sarajedini 2012) to perform the light curve fitting. To summarize the method, **RRFIT** performs a robust search through the user defined parameter space of expected pulsational properties to find the best-fitting light curve template for each star. The program does so by thoroughly searching the defined period space and generating potential light curves based upon the supplied templates at each period using the genetic algorithm, **PIKAIA** (Charbonneau 1995), to optimize each template to fit the data. Each light curve fit is then ranked according to its reduced χ^2 , and the parameters that minimize this value are taken to be the best-fitting light curve.

Given previous studies of the stellar populations and SFH in DDO210, we expect there to be a sizable population of RR Lyrae variables as well as Cepheid variables. Considering this, we performed a first-pass with **RRFIT** on our entire set of variable candidates searching for periods in the range 0.2–1.0 days, which allowed us to distinguish between potential faint, short-period stars and the brighter stars with presumably longer periods. Following this first pass, we divided the sample into two groups by making a cut in F814W at 24.25 mag. Variables fainter than this were taken as RR Lyrae candidates, while brighter variables were assigned as Cepheid candidates.

We then ran a second round of **RRFIT** on each set of variable candidates, this time tailoring the pulsational parameter space to match each type of variable. In the case of the Cepheid candidates, we searched for periods in the range of 0.4–4.0 days, covering the period distributions for the different subclasses of Cepheids found in LG dwarf galaxies. We chose to use the RR Lyrae templates for the Cepheids since the light curve shapes are similar. For the RR Lyrae candidates, we searched for periods in the usual range of 0.2–1.0 days.

Table 1. An example time-series photometry set for one variable star candidate in DDO210. The full set of these for all variable star candidates is included in the online version of the journal.

Star ID	Filter	HJD - 2456000 (days)	Magnitude	Magnitude error
V0003	F475W	471.0488	23.141	0.036
V0003	F814W	471.06405	22.231	0.058
V0003	F475W	471.11204	23.256	0.048
V0003	F814W	471.12809	22.349	0.053
V0003	F475W	471.18299	23.253	0.052
V0003	F814W	471.19824	22.275	0.052
V0003	F475W	471.24499	23.317	0.046
V0003	F814W	471.26104	22.399	0.064
V0003	F475W	471.31594	23.372	0.048
V0003	F814W	471.33119	22.396	0.063
V0003	F475W	471.37795	23.463	0.042
V0003	F814W	471.39401	22.444	0.047
V0003	F475W	471.4489	23.439	0.06
V0003	F814W	471.46414	22.388	0.048
V0003	F475W	471.51092	23.543	0.052
V0003	F814W	471.52697	22.499	0.055
V0003	F475W	471.58185	23.568	0.053
V0003	F814W	471.59709	22.466	0.046
V0003	F475W	471.64388	23.629	0.055
V0003	F814W	471.65993	22.531	0.061
V0003	F475W	472.11366	23.608	0.049
V0003	F814W	472.1289	22.513	0.053
V0003	F475W	472.17573	23.65	0.05
V0003	F814W	472.19179	22.618	0.05
V0003	F475W	472.24661	23.687	0.05
V0003	F814W	472.26185	22.575	0.049
V0003	F475W	472.3087	23.74	0.047
V0003	F814W	472.32475	22.675	0.051
V0003	F475W	472.37956	23.684	0.053
V0003	F814W	472.39481	22.613	0.062
V0003	F475W	472.44166	23.749	0.053
V0003	F814W	472.45772	22.702	0.057
V0003	F475W	472.51251	23.536	0.06
V0003	F814W	472.52776	22.494	0.054
V0003	F475W	472.57461	23.111	0.055
V0003	F814W	472.59067	22.314	0.068
V0003	F475W	473.24368	23.05	0.056
V0003	F814W	473.25892	22.23	0.063
V0003	F475W	473.30586	23.234	0.048
V0003	F814W	473.32192	22.314	0.052
V0003	F475W	473.37662	23.218	0.045
V0003	F814W	473.39187	22.292	0.045
V0003	F475W	473.43881	23.341	0.043
V0003	F814W	473.45487	22.403	0.06
V0003	F475W	473.50957	23.328	0.059
V0003	F814W	473.52482	22.334	0.059
V0003	F475W	473.57178	23.456	0.052
V0003	F814W	473.58783	22.455	0.048

We took advantage of the relationship between pulsation amplitudes in different bandpasses for the RR Lyrae stars as discussed in Dorfi & Feuchtinger (1999) in order to improve the template fitting procedure for these stars. Dorfi & Feuchtinger (1999) provide these relationships in the Johnson–Cousins system for the B, V, and I filters. In order to derive similar transformations for the VEGAMAG photometric system, we used the following technique. First, we generated 4,000 artificial RR Lyrae light curves using the templates in **RRFIT**. These artificial light curves were generated with the following constraint on their amplitudes from

Dorfi & Feuchtinger (1999):

$$A_B = 0.102 + 1.894A_I \quad (2)$$

We then transformed these light curves to the VEGAMAG magnitudes in F475W and F814W using the prescription from Sirianni et al. (2005) at each phase in the light curve. Finally, the amplitudes in F475W and F814W were calculated for each synthetic light curve, and the following linear relation was fit to these amplitudes:

$$A_{F475W} = 0.089 + 1.734A_{F814W} \quad (3)$$

Equation (3) thus provides a constraint on the amplitudes of the RR Lyrae candidates in the VEGAMAG photometric system. We modified RRFIT to implement this constraint in order to improve the accuracy of the RR Lyrae fitting routine. On the other hand, for Cepheids it has been known for some time that the amplitude ratio $A_I/A_V = 0.6$ mag is independent of period or amplitude (Tanvir 1997). However, the findings of Coulson & Caldwell (1989) suggest a possible dependence of A_B/A_V on period, so we did not implement any such amplitude constraint on the Cepheid candidates.

Finally, we performed multiple checks on these best-fitting light curve to assess their validity. For the RR Lyrae stars, the locations in the Bailey (period-amplitude) diagram was checked to verify that each light curve's period, amplitude, and mode follow the well-known behavior of RR Lyrae stars in this space. We manually checked for potential aliasing by visually examining all light curves produced by RRFIT. Light curves with periods suspected to be aliased were checked with the interactive light curve fitting program, FITLC (Mancone & Sarajedini 2008). This software operates on the same principles as RRFIT but provides a GUI for the user to examine the light curves and the period- χ^2 space. This program illustrates the best-fitting light curve for each template overplotted on the data, along with a plot of reduced χ^2 versus period for each template. In this way, FITLC allows one to explore different period/template combinations. Occasionally, the automated fitting routine misclassifies a star or falls victim to a period alias. Aliased periods can be compared with other periods lying at a similar χ^2 minimum. If a fit appears anomalous on the Bailey diagram (e.g. significantly shorter/longer period at a given amplitude compared with the other RR Lyrae stars on the diagram), or a period-folded light curve appears to have a large gap, the fit period is usually aliased with two or more comparable χ^2 minima. Using FITLC, we explored the different periods with similarly low χ^2 for these problematic light curves. If one of these other periods yields light curve parameters that better match the data and/or previously observed behavior for that type of variable (e.g. period-amplitude relation), then that period is taken as the correct one. We will hereafter refer to this procedure as manual fitting.

Stars which failed to pass this vetting procedure with reasonable properties were removed from the sample. This left 107 (75 Cepheid; 32 RR Lyrae) high confidence variable stars in our sample. Manual fitting with FITLC was required for 4 RR Lyrae stars and 7 Cepheids, accounting for 10% of our total pulsating variable sample. The CMD locations of our final variable star sample are shown in Fig. 2. Some example light curves of each of these variables, folded with the best-fitting period, are plotted in Figs. 3 and 4. Properties

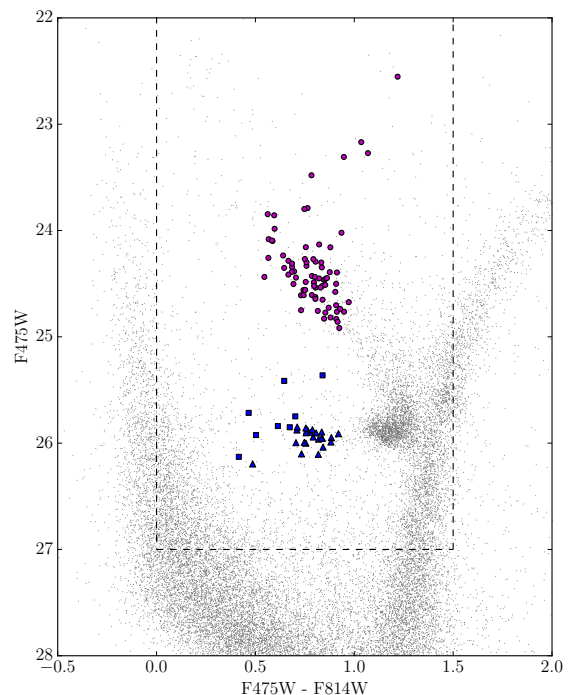


Figure 2. The CMD of DDO210 focusing on the pulsating variable stars. The grey points indicate the entire photometric sample of stars, while the coloured shapes indicate the pulsating variables. Each symbol represents a Cepheid (magenta circles), an RRab star (blue triangles), or an RRC star (blue squares). Phase-averaged mean magnitudes and colours calculated from the best-fitting template light curve are used to plot the variables. The dashed line shows the selection region adopted to find potential pulsating stars.

of each of these candidate pulsators are presented in Table 2.

3.2 Simulations

We performed artificial light curve simulations to assess the accuracy and precision of our automated fitting procedure on this data set (see Ordoñez, Yang, & Sarajedini (2014) and references therein). This involved using the Fourier templates from RRFIT to create artificial light curves. The properties of these artificial light curves were chosen to best represent the types of pulsating variables found in DDO210. We sampled the appropriate period, amplitude, magnitude, and colour ranges in which the RR Lyrae and Cepheids were found to lie. Each of these properties was sampled from a uniform distribution and assigned to each individual light curve. For the artificial RR Lyrae light curves, the amplitude constraint in Equation (3) was applied. Observations on these artificial F475W, F814W light curves were then simulated utilizing the cadence of our dataset and realistic photometric errors.

Unlike the other studies employing these artificial light curve simulations, we have accounted for ranges in magnitude and colour, utilizing the photometric errors as a func-

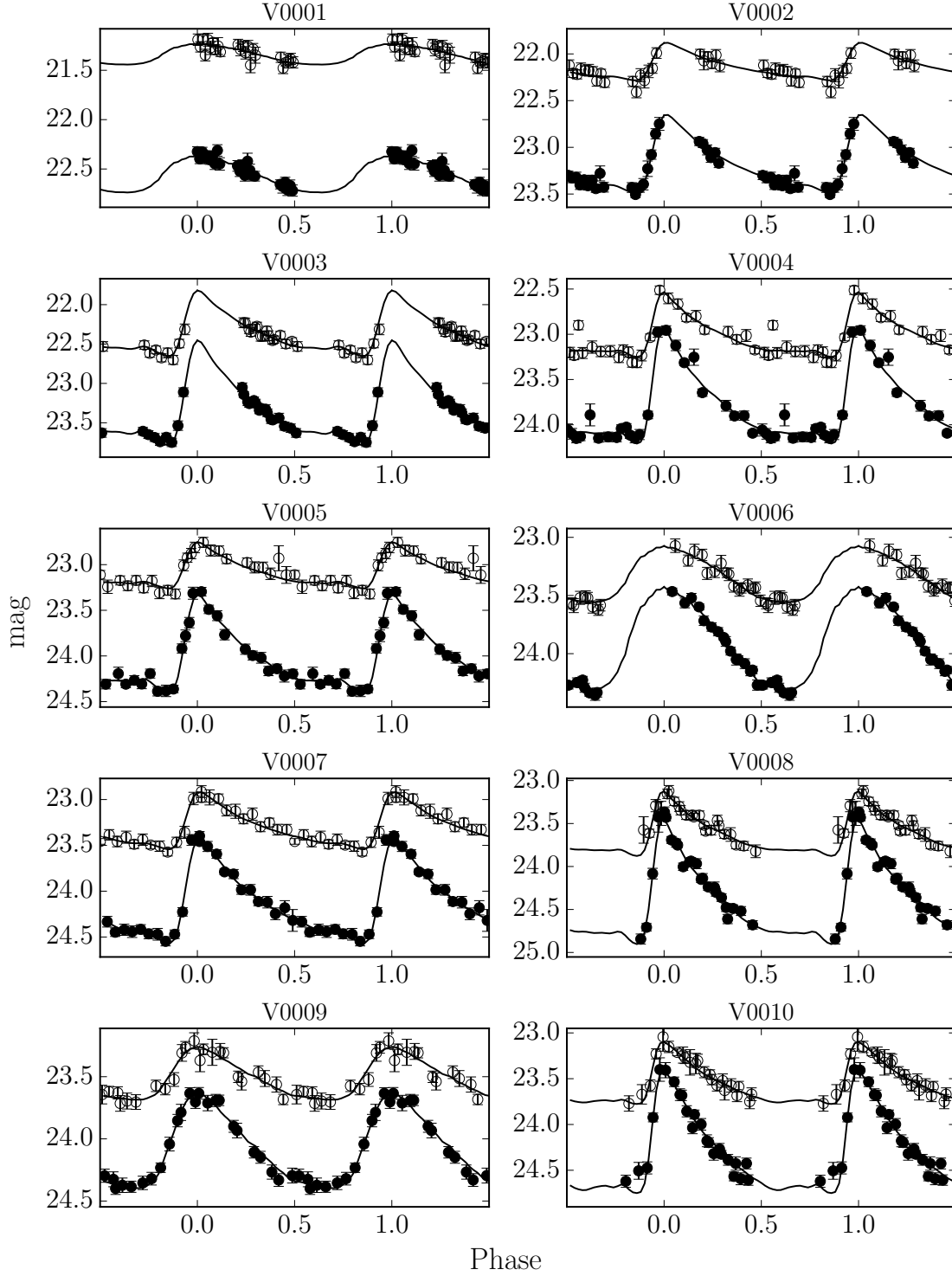


Figure 3. Example light curves of some Cepheid variables in DDO210. Open circles represent F814W observations, while filled circles are F475W observations. The solid lines illustrate the best-fitting templates to each light curve.

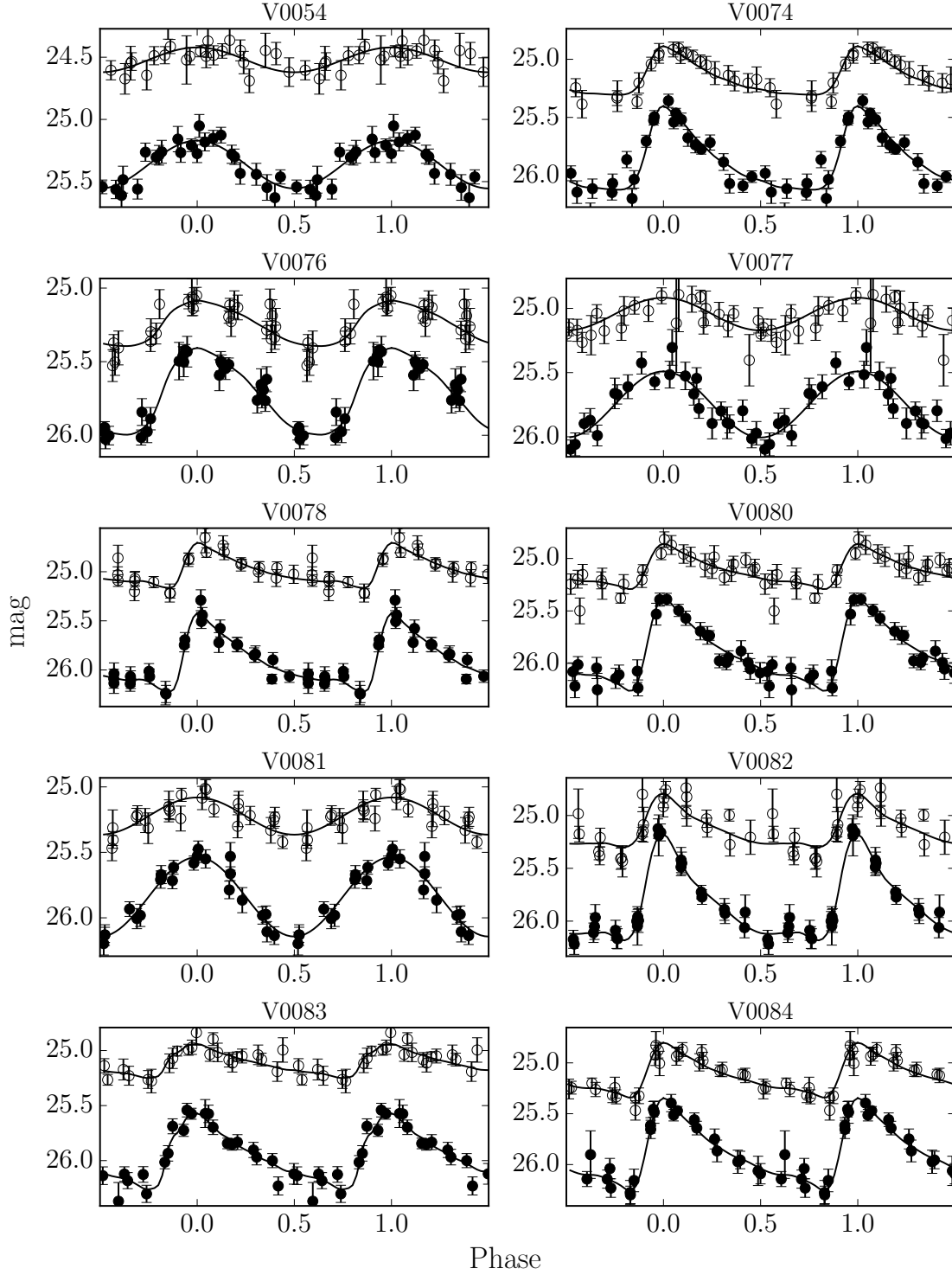


Figure 4. Same as Fig. 3 for some RR Lyrae variables.

tion of magnitude in each the F475W and F814W bands. We modeled the photometric error function as a constant value for bright magnitudes, and an exponential function for fainter magnitudes. This model was then fit to the errors from each individual photometric measurement for every star in our sample. In this way, we were able to realistically assess how our light curve analysis accuracy and completeness vary as a function of magnitude.

Once the simulated observations were generated, we then input these into RRFIT exactly as we did for our real light curves. The difference between the synthetic input and best-fitting light curve parameters for each artificial light curve then gives estimates of the uncertainties inherent in the fitting procedure. We show the results of these simulations for the Cepheid, RRab, and RRC stars in Fig. 5.

Given that these data cover a baseline of ~ 2.5 days, it is expected that periods greater than this to be recovered with significantly less accuracy than for shorter periods. This is clearly visible in the Cepheid simulations. However, for periods shorter than 2.5 days, the period errors remain constant and reasonably small. Only 3 of the 75 Cepheid candidates were fit with periods longer than 2.5 days, and the longest period Cepheid (5.15 days) was fit manually in FITLC since it fell outside of the explored period range. Therefore, we expect the observing baseline to affect the periods of only 2 out of the 107 variables in our sample.

To gauge the quantitative uncertainties inherent in the fitting routine from these simulations, we perform the following statistical test discussed in Ordoñez et al. (2014). From our sample of artificial light curves, we sample the corresponding number of identified stars (75 Cepheid; 24 RRab; 8 RRC) and calculate the average error in the light curve parameters (ΔP , ΔA_{F475W} , etc.). This sampling is repeated 10,000 times to build a statistical distribution of the expected errors. These distributions then represent good estimators for the systematic and random errors inherent in the fitting procedure. Specifically, the peak of the distribution reveals any systematic errors, and the spread estimates the random uncertainties (standard error) in each parameter. Gaussian fits to the final error distributions therefore yield our fiducial uncertainty values. These uncertainties are presented in Table 3 for each type of simulated variable. Since only 2 Cepheids will be affected by the large uncertainties at $P > 2.5$ days, we restricted this test to artificial light curves with periods less than this value.

We conclude this section by pointing out that for most of the simulated light curve parameters, the systematic errors are smaller than the random errors. However, the simulations reveal that we may be underestimating the amplitudes for the Cepheid and RRab light curves by 0.02 and 0.04 mag, respectively. We tested to see if this affected the metallicity estimates for the RRab stars (see Section 4.1) by subtracting this offset from the amplitudes, and it turned out to drive the metallicity estimates higher by ~ 0.05 dex. Considering that this is smaller than the other sources of uncertainty for this calculation, we do not expect these errors to impact the main results of this paper significantly.

4 RR LYRAE STARS

The relative paucity of RR Lyrae stars in DDO210, especially compared with the younger Cepheids, is fully consistent with the appearance of its CMD. The red HB morphology and strong red clump (RC) in this galaxy indicate a younger average age for the stellar population. The small number of RR Lyrae stars implies a weaker star formation rate at times $\gtrsim 10$ Gyr ago, which is fully consistent with the appearance of the other features. This agrees well with the synthetic CMD, SFH analysis of Cole et al. (2014). Their Fig. 4 shows a distinct minimum just before a lookback time of 10 Gyr.

4.1 Metallicity of RRab stars

In addition to providing insights into the SFH of a galaxy, the RR Lyrae stars also inform us regarding the chemical enrichment of their host system through their metallicity distribution function (MDF). As discussed in Section 1, many studies have provided methods of calculating an iron abundance, $[\text{Fe}/\text{H}]$, from the shape of the light curves of RR Lyrae stars. Considering that the dataset employed in this study is not well-suited for a Fourier analysis on each light curve, we utilized the relation of Alcock et al. (2000) to calculate $[\text{Fe}/\text{H}]$ for each individual RRab star:

$$[\text{Fe}/\text{H}] = -8.85[\log P_{ab} + 0.15A_V] - 2.60 \quad (4)$$

Since we did not have V band imaging for these stars, we opted to estimate A_V for each RRab star using the relation between A_B and A_I from Dorfi & Feuchtinger (1999).

Fig. 6 shows the RRab MDF calculated using both the I -band and B -band amplitudes. The MDFs show no significant difference, and the mean metallicity in each case is $\langle [\text{Fe}/\text{H}] \rangle = -1.65 \pm 0.11$ dex using A_I and $\langle [\text{Fe}/\text{H}] \rangle = -1.61 \pm 0.11$ dex using A_B , both in full agreement. We thus take a singular estimate by averaging these two values together to obtain $\langle [\text{Fe}/\text{H}] \rangle = -1.63 \pm 0.11$ dex. Assuming the effects of α -enhancement are small, this also agrees with the AMR from the synthetic CMD analysis of Cole et al. (2014). Their Fig. 5 shows this AMR, and at a lookback time of approximately 11 Gyr, this average metallicity is $[\text{M}/\text{H}] \sim -1.7$ dex. The RRab stars, which formed at approximately this time, support the results of the analysis of Cole et al. (2014).

4.2 Bailey diagram

An important diagnostic of an RR Lyrae population is the Bailey (period-amplitude) diagram. We show this for the 32 RR Lyrae stars within DDO210 in Fig. 7. Also plotted in this figure are the loci for the two different Oosterhoff populations in the Galactic globular clusters (GGCs) from Cacciari, Corwin, & Carney (2005). While most of the RRab stars lie around the Oosterhoff type I (OoI) locus, their mean period $\langle P \rangle = 0.609 \pm 0.011$ d and mean metallicity $\langle [\text{Fe}/\text{H}] \rangle = -1.63 \pm 0.11$ dex place this galaxy in the so-called Oosterhoff gap, along with the majority of dSph galaxies. Additionally, the first-overtone to fundamental mode population ratio, $(\text{RRc})/(\text{RRc} + \text{RRab}) = 0.25$, is consistent with an Oosterhoff-intermediate classification for this galaxy.

The discrepancy between the appearance of the Bailey diagram and the other Oosterhoff classification methods

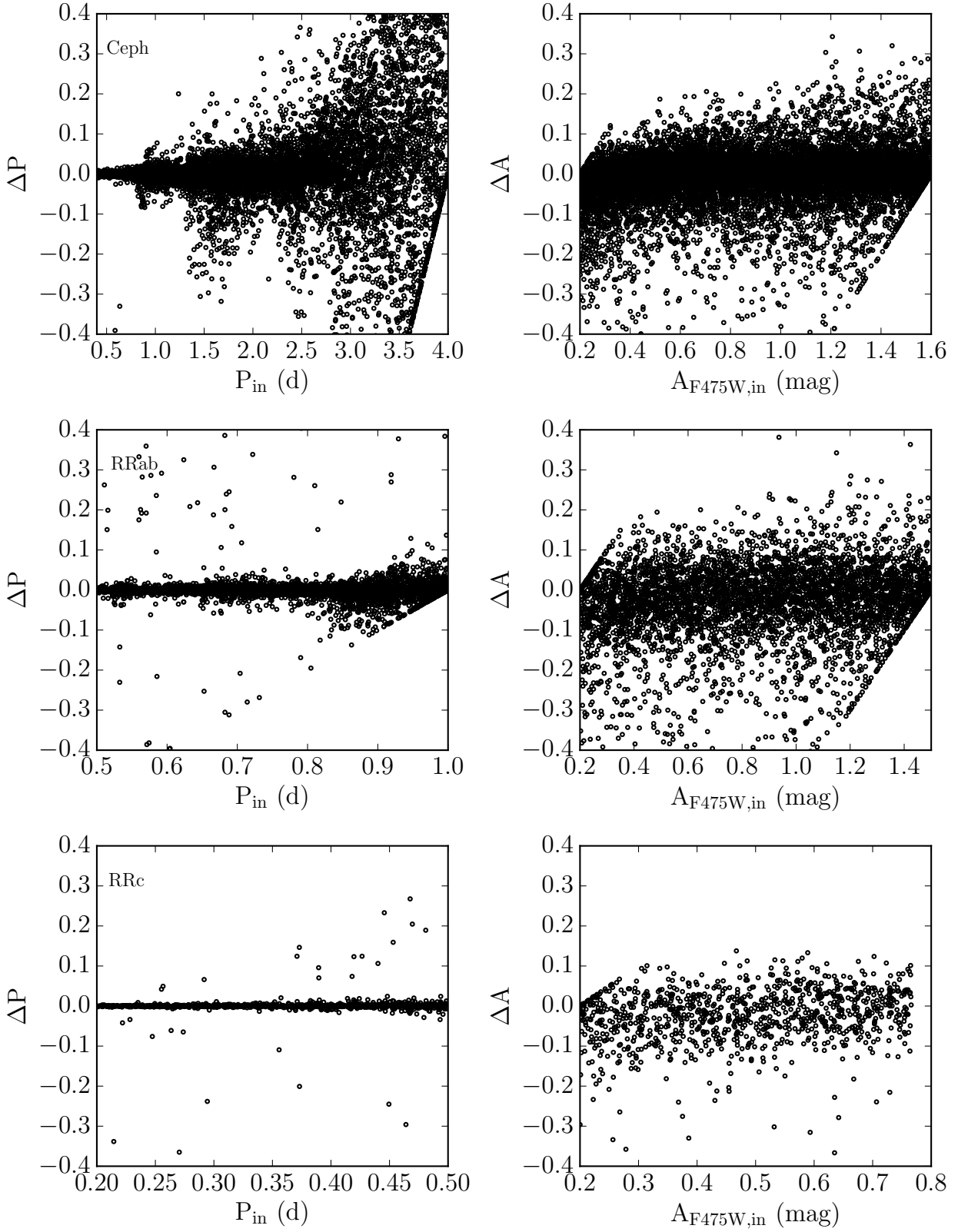
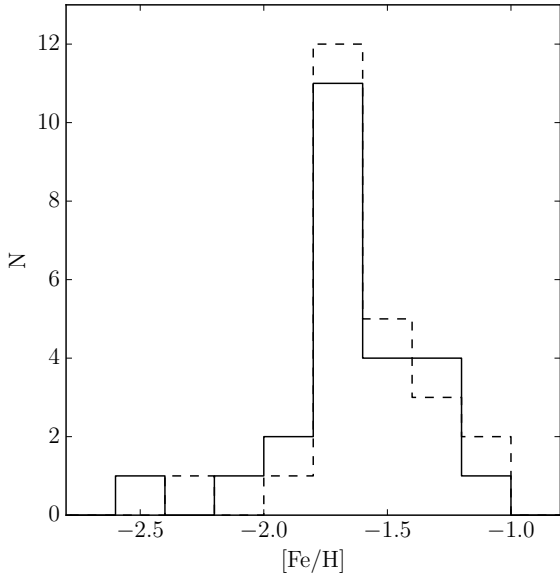
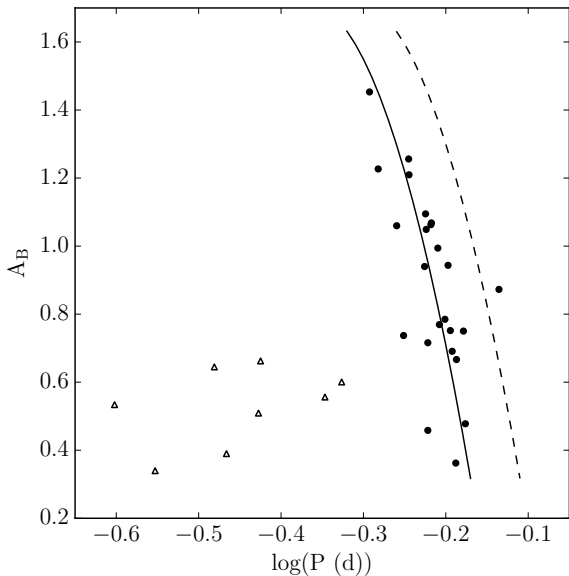


Figure 5. Results of the light curve simulations. The left panels show the period error as a function of input period, while the right panels show the amplitude error versus input F475W amplitude.

Table 3. Uncertainties estimated from the light curve simulations.

Variable	$\sigma_{P,\text{systematic}}$ (d)	$\sigma_{P,\text{random}}$ (d)	$\sigma_{AF475W,\text{systematic}}$ (mag)	$\sigma_{AF475W,\text{random}}$ (mag)	$\sigma_{mF475W,\text{systematic}}$ (mag)	$\sigma_{mF475W,\text{random}}$ (mag)
Cepheid	-0.0044	0.0058	-0.0233	0.0103	-0.0004	0.0043
RRab	-0.0011	0.0042	-0.0399	0.0257	0.0049	0.0103
RRc	0.0007	0.0026	-0.0213	0.0228	-0.0022	0.0073

**Figure 6.** The MDF of the RRab stars using the relation of Alcock et al. (2000) to calculate the metallicities. The solid line represents the MDF calculated converting A_I to A_V . The dashed line is the same but estimating A_V from A_B .**Figure 7.** The Bailey diagram for the RR Lyrae stars in DDO210. RRab stars are represented as filled circles, while the open triangle represent the RRc stars. Plotted as the solid and dashed lines are the Oosterhoff I and II trend lines from Cacciari et al. (2005).

have been noted in previous studies (Ordoñez et al. 2014; Stetson 2014). Stetson (2014); Fiorentino et al. (2015) discuss this issue in detail, and conclude that the absence of high-amplitude, short-period (HASP) RRab stars in dSph and ultra-faint dwarf (UFD) galaxies present a fundamental difference between the ancient RR Lyrae population in dSph/UFDs and those in the GGCs and Galactic Halo. This HASP absence, which Fiorentino et al. (2015) attribute to the metal-poor environments forming the RR Lyrae stars, skews the mean RRab period to longer values. Therefore, it seems that DDO210 hosts an RR Lyrae population similar to the dSph and UFDs in the LG owing to their similarly metal-poor environments at early ages.

4.3 Distance to RRab stars

The distance to DDO210 has been a matter of some debate since its discovery. Most recent distance estimates to this galaxy using the TRGB place DDO210 at a distance modulus of $\mu \sim 25$ (McConnachie et al. 2005; Jacobs et al. 2009), and the most recent synthetic CMD analysis by Cole et al. (2014) report a distance modulus of $\mu = 24.95 \pm 0.10$. We now compute the distance to DDO210 using the period-luminosity-metallicity (PLZ) relation from Catelan et al. (2004):

$$M_I = 0.471 - 1.132 \log P + 0.205 \log Z \quad (5)$$

Using the RRab metallicities from Section 4.1 calculated with the I -band amplitudes, we convert to $\log Z$ using the following relation: $\log Z = [Fe/H] - 1.765$ to remain consistent with Catelan et al. (2004). Again, here we have not corrected for the effects of α -enhancement in the absence of a strong constraint for $[\alpha/Fe]$ for these stars. Apparent mean magnitudes of these RRab stars have been corrected for extinction using $A_I = 0.076$ mag from Schlafly & Finkbeiner (2011) for DDO210 retrieved from NED².

The mean distance modulus of the RRab stars calculated in this way is $\mu = 25.07 \pm 0.12$ where the error bar represents one standard deviation. We note that the effects of different helium abundances on this RR Lyrae PLZ relation have not been fully explored, and significant helium abundance in the DDO210 RR Lyrae stars could present a significant systematic error in this distance determination. There may also be some systematic error resulting from α -enhancement when calculating $\log Z$. Even considering these uncertainties, our RR Lyrae distance is roughly consistent with other distance determinations to this galaxy within the uncertainties. The RR Lyrae distance does however seem to lie on the farther end of the distribution of previous distance measurements. In fact, our distance is closer to that of McConnachie et al. (2005) ($\mu = 25.15 \pm 0.08$).

² <https://ned.ipac.caltech.edu/>

4.4 Peculiar RR Lyrae candidates

We now turn to discussing a few anomalous RR Lyrae candidates within our sample. The CMD of DDO210 in Fig. 2 shows two bright outliers in the RR Lyrae population near $m_{F475W} = 25.4$ mag and colours of $(F475W - F814W) = 0.6$ and $(F475W - F814W) = 0.8$ mag. Neither of these RRc stars appear as outliers in the Bailey diagram, nor do they display anomalous light curves. It is evident from Fig. 2 that most of the RR Lyrae candidates that we identified occupy the expected region in the CMD, except for the two aforementioned bright outliers lie clearly brighter the HB. In fact, these stars appear to lie in between the bulk RR Lyrae population and the Cepheids. It is possible that these stars are faint ACs, but this seems unlikely given their separation from the bulk Cepheid population in the CMD and PL relations (see Section 5 for a full discussion of the Cepheids). We also considered the possibility that these stars are type II Cepheids (BL Her) stars, but ruled this out because BL Her stars generally have periods between 1 and 4 days (these outliers both have periods near 0.4 days). Another possibility is that these stars contain unresolved companions, making them appear brighter. This is more likely the case as Cepheids with such short periods are uncommon.

One more peculiar RR Lyrae candidate deserves discussion. Immediately apparent upon examining Fig. 7 is the one outlying RRab star near the OoII locus. The longest period RR Lyrae in our sample, this star is also the most metal-poor RRab star. While it is tempting to discard this star as a contaminating Type II or anomalous Cepheid, we note that this star lies right on the HB ($m_{F475W} = 25.91$ mag) in the CMD near the red end of the RR Lyrae gap. It may therefore be a very metal-poor RR Lyrae star formed within DDO210. Considering once again the analysis of Cole et al. (2014) for comparison, we see that the AMR for the galaxy has the largest metallicity dispersion at a lookback time of 11 Gyr, corresponding to the age of the RR Lyrae stars. In fact, the rms metallicity range for that time bin extends down to metallicities of $[M/H] = -2.5$ dex. Therefore, such a metal-poor RR Lyrae star is not inconsistent with the synthetic CMD analysis of Cole et al. (2014).

5 CEPHEIDS: ANOMALOUS OR CLASSICAL?

5.1 Comparison with evolutionary tracks

The Cepheid variables dominate the pulsators found in DDO210. However, as other authors have pointed out (Fiorentino et al. 2012), this region of the CMD hosting these stars is degenerate. That is to say that stellar populations with different masses and metallicities can occupy this region, including the Cepheid instability strip. In low-metallicity environments, this makes distinction between these different populations difficult. We note that no Cepheids with periods longer than ~ 5 days were identified in our data. Given the quality of the data at these bright magnitudes, we expect to flag variability at these longer periods even with incomplete phase coverage. Therefore, this absence of longer period Cepheids is more likely a reflection of the Cepheid population itself rather than an observational bias.

To further complicate matters, recent investigations of the Cepheid populations in dwarf galaxies have revealed that

the distinction between ACs and CCs is not as clear as once thought. These studies have found that the period and luminosity distributions of these two types of variables can overlap, making a separation based on this diagram alone difficult (Gallart et al. 2004; Fiorentino et al. 2012; Clementini et al. 2012; Bernard et al. 2013; Stetson 2014). One other way to potentially distinguish between a population of CCs and ACs is to utilize our theoretical understanding of ACs. Since ACs are stars with masses less than the transition mass between partial-degenerate, central He burning and quiescent central He burning, one can compare the positions of stellar evolutionary tracks near this mass ($\sim 2.1 M_{\odot}$ for $[Fe/H] \leq 0.7$ dex) with the observed Cepheid population (Fiorentino et al. 2012).

We have performed this analysis for the Cepheids in DDO210, and the results are shown in Fig. 8. This shows the CMD of DDO210 highlighting the Cepheid variables. The magnitudes have been converted to absolute magnitudes using the RR Lyrae distance modulus from Section 4.3, and colours de-reddened using the reddening to DDO210 from Schlafly & Finkbeiner (2011). To attempt to deduce the nature of the Cepheids in DDO210, we have plotted the He-burning stages of the canonical, scaled-solar evolutionary tracks for stars of different masses (1.8, 2.1, 2.8, 3.0, 3.5, and $5.0 M_{\odot}$; coloured lines in 8) and two different metallicities ($[Fe/H] = -1.5$ dex and $[Fe/H] = -1.3$ dex; left and right panels in Fig. 8, respectively) from the BaSTI stellar evolutionary library (Pietrinferni et al. 2004). We did not explore lower metallicities because such stars are deemed unlikely to have been formed within the past 6 Gyr considering the AMR from Cole et al. (2014). On the other hand, ACs are not expected to reach metallicities above $[Fe/H] = -1.3$ dex because they do not enter the instability strip above this metallicity, so higher metallicity tracks were not explored either.

From Fig. 8, it is evident that the brighter Cepheids in this galaxy are clearly CCs, irrespective of the metallicity adopted for these stars. We have identified these stars as lying near or brighter than the $2.8 M_{\odot}$ track in both cases (the triangles in Fig. 8). The remaining Cepheids cluster around the $2.1 M_{\odot}$ track for the lower metallicity case but not the higher metallicity case. Thus, we are presented with a situation similar to what Fiorentino et al. (2012) found in Leo I. That is, the nature of the Cepheids in DDO210 seems to depend on the metallicity of these stars. If they are sufficiently metal-poor, which Kirby et al. (2013) indicate is possible calculating $\langle [Fe/H] \rangle = -1.44$ dex for DDO210, it is likely that many of the fainter Cepheids are ACs. On the other hand, if these stars are all characterized by a slightly higher metallicity, as is suggested by the AMR of Cole et al. (2014) for ages ≤ 6 Gyr, then these Cepheids should all be CCs.

5.2 PL relations

The locations of these stars in the CMD coupled with the AMR from Cole et al. (2014) indicate that most if not all of these stars are in fact CCs. In an attempt to place further constraints on the nature of these Cepheids, we show the M_B and reddening-free, Wesenheit PL relations in Fig. 9. Again, we have used the RR Lyrae distance modulus and extinctions as before to convert to absolute magnitudes. We have

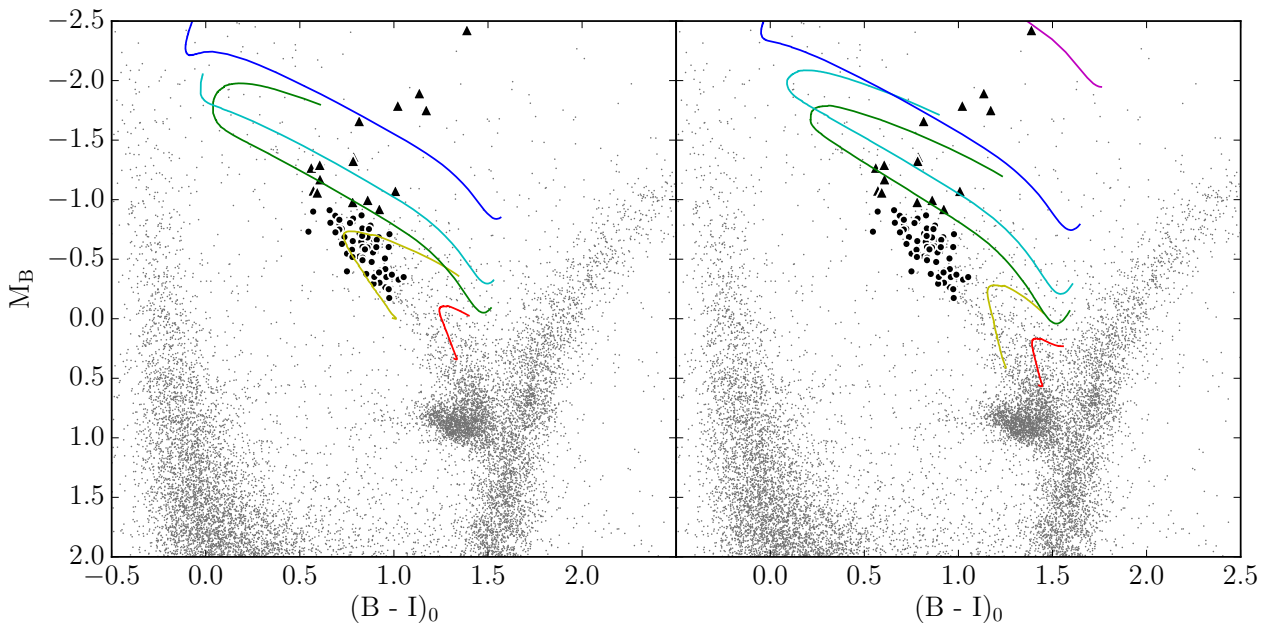


Figure 8. *Left:* The CMD of DDO210 comparing Cepheid variables (black circles and triangles) with BaSTI He-burning, stellar evolutionary tracks (red to magenta: 1.8, 2.1, 2.8, 3.0, 3.5, and 5.0 M_{\odot}) for $[\text{Fe}/\text{H}] = -1.5$ dex. The triangles show Cepheids that are very likely CCs, while the filled circles show Cepheids that may be either ACs or CCs. *Right:* Same as the left panel but with $[\text{Fe}/\text{H}] = -1.3$ dex evolutionary tracks of the same masses.

taken several PL relations from the literature for CCs and ACs to compare with the Cepheids in DDO210. For the CCs, we use the B -band PL relation from Gallart et al. (2004) for short-period CCs. As for the ACs, we use the B -band PL relation from Pritzl et al. (2002). Although there is a considerable amount of scatter, it appears that the likely CCs identified using Fig. 8 (triangles in Fig. 9; see Section 5.1) do follow the CC PL relations. As for the fainter Cepheids, the picture is again unclear. The faintest of these do seem to aggregate near the AC PL relations, but there is enough scatter to confuse the distinction for most of them.

The Wesenheit magnitudes inherently remove the effects of reddening to stars (Brodie & Madore 1980). To calculate Wesenheit magnitudes, we use the following equation:

$$W_B = M_B - R(B - I)_0 \quad (6)$$

Here, R is the ratio of total-to-selective absorption, $A_B/E(B-I) = 1.710$ (Schlafly & Finkbeiner 2011). We have constructed W_B PL relations using the B -band PL relations previously mentioned combined with the I -band relations of Fiorentino et al. (2006) for the ACs, Udalski et al. (1999) for the fundamental mode CCs, and Soszynski et al. (2008) for the first-overtone CCs. We note that we needed to place the first-overtone CC PL relation on the same scale as the fundamental mode one by subtracting 18.449 mag from the first-overtone CC PL relation of Soszynski et al. (2008). This was necessary because this PL relation was not corrected for reddening, but Udalski et al. (1999) did not provide a first-overtone PL relation. Thus, subtracting the difference between the fundamental mode zero-points of Soszynski et al. (2008) and Udalski et al. (1999) places the first-overtone M_I PL relation on the same scale as the fundamental mode one. To construct the Wesenheit PL relation for the different

types of Cepheids, we took the B and I PL relations at a given period, and calculated W_B using Equation (6).

The result, shown in the right panel of Fig. 9, has clearly reduced the scatter in the DDO210 Cepheid PL relation. While these two PL relations lie close in this Wesenheit plane, it appears that most of the Cepheids lie brighter than the AC PL relations and closer to the CC PL relations in this plane. Additionally, we observe the possible AC candidates (circles) as determined by the CMD analysis in Section 5.1 to lie on the same PL relation for the likely CCs (stars) extended to fainter magnitudes. This would seem to support this Cepheid population containing mostly, if not entirely, CCs. Finally, we draw attention to the two bright outliers on the short-period end of the W_B PL relation. These stars are more likely second-overtone Cepheids since these pulsators have been observed to pulsate with shorter periods at a given magnitude when compared to the first-overtone pulsators.

5.3 Specific frequency of Anomalous Cepheids

The final test we perform to discern the nature of the Cepheids in DDO210 is to examine the specific frequency of the potential ACs. Mateo, Fischer, & Krzemiński (1995) first noted that the specific frequency of ACs (number per $10^5 L_{V,\odot}$) is strongly correlated with both the absolute visual magnitude and mean metallicity of MW satellite dSph. Pritzl et al. (2004, 2005) further extended the study of ACs to dSph orbiting M31 and discovered those galaxies to follow the same trends. Pritzl et al. (2005) also note that Phoenix, a dTrans, follows the same trends as the dSph, indicating that these relations may hold independent of galaxy morphological type.

If we assume that this relation holds for all dwarf galax-

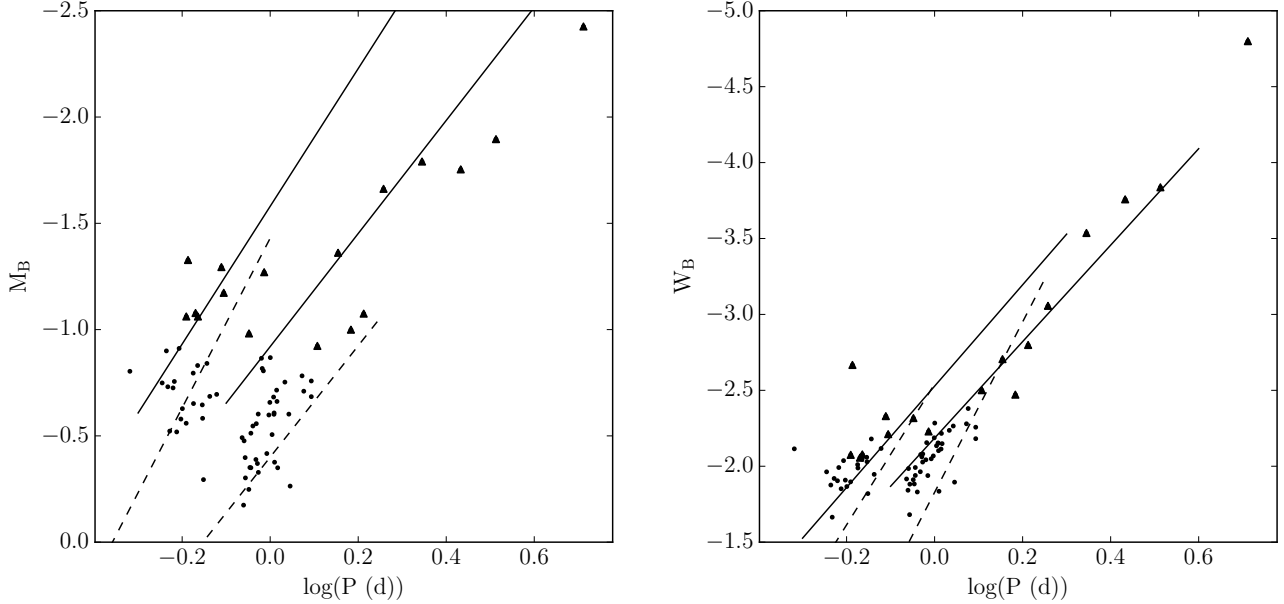


Figure 9. *Left:* The B -band PL relation for the Cepheids in DDO210. The solid lines are the PL relations for fundamental and first-overtone, short-period CCs from Gallart et al. (2004). The dashed lines are the PL relations for ACs from Pritzl et al. (2002). Symbols for the points are as in Fig. 8. *Right:* The Wesenheit PL relation for the Cepheids in DDO210.

ies in the LG, then we expect the specific frequency of ACs in DDO210 to follow these same trends. We have therefore calculated the AC specific frequency in DDO210 assuming all of the 58 potential ACs identified in Section 5.1 are bona fide ACs. For this calculation, we have used an absolute magnitude of $M_V = -10.58$ mag (McConnachie et al. 2006), a surveyed area fraction for this dataset of 50% (Cole et al. 2014), and mean metal abundance of $[Fe/H] = -1.44$ dex (Kirby et al. 2013). We compare the AC specific frequency of DDO210 with the other dwarf galaxies in Fig. 10.

Clearly, DDO210 does not follow the same AC specific frequency trends as other LG dwarfs if we assume all potential ACs to be real. In fact, for DDO210 to fall in line with the trend for other dwarfs, our sample of Cepheids would need to contain $\lesssim 2$ ACs. Thus, we are left with two scenarios: 1) Most or all of these AC candidates are indeed true ACs, and the specific frequency trends do not hold for all dwarfs, or 2) The specific frequency trends do hold for DDO210, and only $\lesssim 2$ of these Cepheids are in fact ACs. Scenario 2) coupled with the AMR of Cole et al. (2014), the locations of the Cepheids in the CMD, and the Wesenheit PL relations for these Cepheids lead us to conclude that the majority of the Cepheids in this galaxy are CCs.

6 DISCUSSION

The main goal of this work was to investigate the properties of the pulsating variables in the context of the SFH of DDO210. The recent SFH analysis of Cole et al. (2014) provides an excellent comparison to this end. As we have already discussed, the metallicity of the RR Lyrae stars derived in this work agrees well with the AMR from Cole et al. (2014) at ages of ~ 11 Gyr, but is inconsistent with their AMR for ages $\gtrsim 12.5$ Gyr. Interestingly, their SFH shows a

deep minimum in star formation rate at this 11 Gyr time bin. Those authors note that this drop is robust, and that the star formation rate at this time is only nonzero at the $\sim 2\sigma$ level. The presence of an RR Lyrae population with a mean metallicity of $\langle [Fe/H] \rangle = -1.63 \pm 0.11$ confirms a weak, but nonzero star formation rate during this early epoch in DDO210.

We now turn to discussing our results on the context of massive galactic halo formation. The paradigm for the formation of the MW halo has held that a large part of it has formed through the accretion of dwarf galaxies closely resembling those found in the LG today. Extending this mechanism to other massive galaxies similar to the MW, it follows that the LG dwarfs should provide excellent windows to the systems that built many massive galaxies in general. However, as was pointed out in Section 4.2, the RR Lyrae populations in the dSph and UFDs of the LG appear fundamentally different than those found in the MW halo and GGCs. Fiorentino et al. (2015) attribute this difference to a difference in the metallicity of the ancient stellar populations from which the RR Lyraes formed. They show that the dSph and UFDs did not chemically enrich rapidly enough to produce the HASP RRab stars observed in the Galactic halo, GGCs, and more massive dwarfs like the LMC and Sgr. They find that galaxies need to have enriched to metallicities of $[Fe/H] = -1.5$ dex or more before ~ 10 Gyr in order to produce these HASP RRab stars.

DDO210 appears to harbor an RR Lyrae population lacking in HASP RRab stars, similar to the dSph and UFDs. That these stars are metal-poor of the HASP threshold ($[Fe/H] = -1.63 \pm 0.11$ dex; see Section 4.1) is in agreement with the picture provided by Fiorentino et al. (2015). Those authors go on to estimate that no more than $\sim 50\%$ of the Galactic halo mass could have accreted from these low-mass, metal-poor galaxies. Therefore, it is still possible

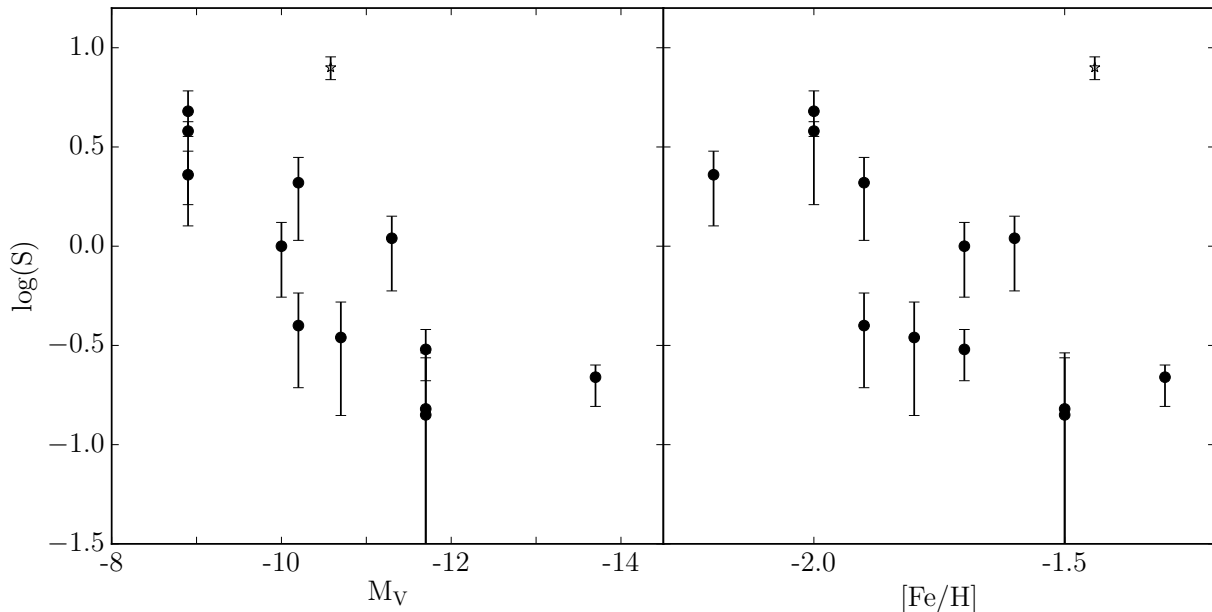


Figure 10. The AC specific frequency trends with absolute visual magnitude and mean metal abundance for LG dwarfs. Error bars are calculated by assuming Poisson statistics govern the errors in the AC counts. The open star shows where DDO210 lies if all of the potential ACs are true ACs. Data for other LG dwarfs from Pritzl et al. (2004, 2005).

that some galaxies resembling DDO210 could be buried in the Galactic halo. However, it seems that the contribution of isolated, low-luminosity dTrans like DDO210 is at a similar level to that of the dSph and UFDs. Considering the low level of early star-formation implied by the RR Lyrae population and the isolation of DDO210, we conclude that galaxies resembling this one probably did not contribute a significant amount of mass to the Galactic halo.

Regarding the Cepheids, it is difficult to place strong constraints on the SFH from our sample given the unknown composition (ACs vs CCs?). We have shown that most of this sample is likely CC, implying that these stars formed within the past 500 Myr or so. To test this hypothesis further, we have applied the period-age relation from Bono et al. (2005) to our sample of Cepheids. Unfortunately, that study did not extend their exploration to metallicities as low as DDO210. Nevertheless, we continue with their most metal-poor period-age relation ($Z = 0.004$) in an effort to gain rough insight into the ages of these stars. The two period-age relations for the fundamental and first-overtone Cepheids take the form:

$$\log t = 8.49 - 0.79 \log P \quad (7)$$

$$\log t = 8.41 - 1.07 \log P \quad (8)$$

Here, t is the age of the Cepheid in years. We used the Wesenheit PL relation (See Section 5.2) in order to distinguish between fundamental and first-overtone Cepheids. Applying Equations (7) and (8) to these sets of Cepheids produced the age distribution shown in Fig. 11. This distribution indicates that, if these stars are all CCs, then these stars all likely formed within the past Gyr. Thus, we can compare these stars' properties with the SFH of Cole et al. (2014) again. If we assume for the sake of comparison that the errors in-

duced by using a period-age relation for more metal-rich stars are relatively small ($\lesssim 100$ Myr), then it seems that most of these stars were born around 300 Myr ago. Cole et al. (2014) examine the SFH of the past 1 Gyr in detail, and they find an enhancement in star formation rate at ages of 250-300 Myr. Thus under these assumptions, the properties of these CC candidates is fully consistent with their synthetic CMD analysis. We note that these ages are also in agreement with the analysis of McConnachie et al. (2006) where they compare theoretical isochrones to the position of the blue-loop stars on their V , $(V - I)$ CMD. They find many of the blue-loop stars in DDO210 in the same region as our Cepheid sample to be ~ 300 Myr old.

The presence of stellar population gradients has been found to be a common characteristic of dwarf galaxies. In the case of DDO210, McConnachie et al. (2006) trace the distribution of different stellar populations and find that the radial profile of the young stars is different from the older RC and RGB stars. In particular, they find the youngest stars to be confined to a small (~ 0.3 kpc) clump roughly one arcminute east of the centre of DDO210. We attempt to further examine this young star distribution through the radial distribution of the age of the Cepheids. In order to estimate where the clump of young stars lies in our data, we took the centroid of all of the Cepheids younger than 250 Myr as our fiducial centre. The projected distances (assuming a distance modulus calculated by the RR Lyrae stars) of the Cepheids from this point are plotted against their ages in Fig. 12, and it reveals that the youngest Cepheids are concentrated to within 0.4 kpc, consistent with the results of McConnachie et al. (2006). On the other hand, Cepheids older than 200 Myr extend almost twice that range in distance.

This point is further illustrated in Fig. 13, where we have plotted the 2σ error ellipses for the mean positions

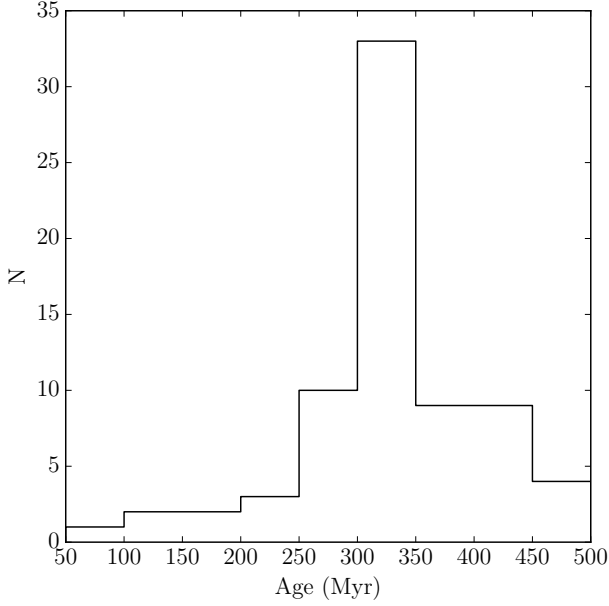


Figure 11. The age distribution of the Cepheid variables in DDO210.

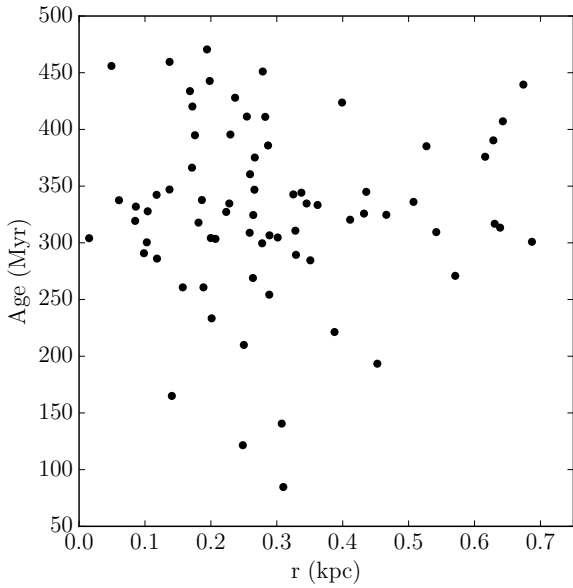


Figure 12. The age of the Cepheid variables in DDO210 versus the radial distance from the centre of the young stars in the galaxy. It is striking to note that no stars younger than ~ 200 Myr are found beyond 0.3 kpc from the centre.

of each variable star population. This plot shows that even with their larger error ellipse (owing to their small number and wide spatial distribution), the young Cepheids are significantly offset from the center of the galaxy and most of the other variable stellar populations. Meanwhile, the older variables, namely Cepheids older than 250 Myr and the RR Lyrae stars, are within 2σ of the center of DDO210. The young Cepheid centroid is $\sim 28''$ (~ 140 pc) from the centre

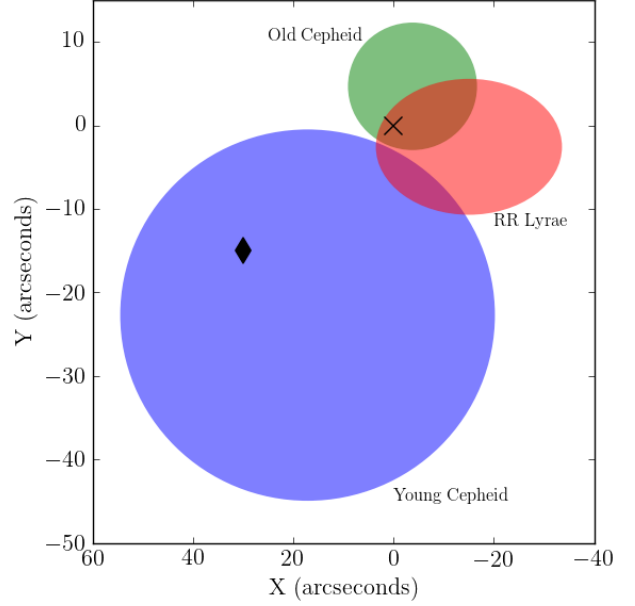


Figure 13. The error ellipses for the mean positions of each variable star population on the sky. The young Cepheids are those that are younger than 250 Myr, and the old Cepheids are older than this age. Each ellipse represents the 2σ error ellipse for each mean position in RA and Dec, where 1σ is the standard error for each mean. The black cross is the center of DDO210 from NED, while the black diamond is the approximate center of the H I 'dent' from McConnachie et al. (2006). North is up, east is to the left.

Table 4. Mean positions and standard errors for each variable population.

Variable type	RA ($^{\circ}$)	Dec ($^{\circ}$)
Young Cepheid	311.7206 ± 0.0052	-12.8542 ± 0.0031
Old Cepheid	311.7148 ± 0.0018	-12.8466 ± 0.0011
RR Lyrae	311.7117 ± 0.0026	-12.8486 ± 0.0011

of DDO210, while the older Cepheid centroid lies only $\sim 6''$ (~ 30 pc) from the centre. The mean positions and standard errors used to construct Fig. 13 are provided in Table 4.

Interpretation of Fig. 13 is somewhat difficult with information available to us. This may indicate that the recent star formation has migrated away from the centre of the galaxy. Indeed, McConnachie et al. (2006) already suggested that such a scenario may have occurred within DDO210 through the process described by Dohm-Palmer et al. (2002) for Sextans A. To summarize the mechanism, star formation is induced on one edge of a gas cloud and thought to migrate through the cloud from instabilities triggered by the supernova and wind-driven shocks of the previous, adjacent star formation episodes. The Cepheids appear consistent with such a scenario occurring with DDO210, and in fact the centre of the youngest Cepheids in our sample lies $\sim 15''$ (~ 70 pc) from the approximate centre of the young stars and corresponding H I 'dent' (black diamond in Fig. 13) discussed in McConnachie et al. (2006). On the other hand, the centre

of the older Cepheids in our sample lies much further from the centre of the young stars from McConnachie et al. (2006) at $\sim 38''$ (~ 180 pc).

As McConnachie et al. (2006) point out, there are other alternatives to explain the offset of the young stars from the galactic centre. For instance, it is possible that DDO210 interacted with some nearby system which could have potentially induced star formation away from the centre. However, the isolation of this galaxy renders this scenario rather unlikely. Another possibility that McConnachie et al. (2006) suggest is the recent capture of gas. However, if this mechanism was responsible for the formation of the youngest stars, then one would not necessarily expect the metallicity of these youngest stars to be similar to the older Cepheids unrelated to this captured gas. The fact that these Cepheids all appear to constitute one continuous population in the CMD and PL plane indicate that they must be of similar chemical composition, and therefore formed from related star formation events.

Finally, another scenario one might imagine to explain the spatial distribution of Cepheids in this galaxy is one in which all of these stars formed off-centre. In this case, the older Cepheids will have had more time to migrate from the original site of star formation. During this dispersal, the older stars have more time to be affected by the overall galactic potential, thereby orbiting the galactic centre as opposed to the natal star forming region. In the absence of any kinematic information for these stars, we cannot confirm this scenario. We do however note that recent theoretical work has shown that significant radial stellar migration in dwarf galaxies is not expected to occur over these short time-scales (Schroyen et al. 2013).

We should also note that such migrating star formation regions appear to occur within systems marked by solid-body rotation (Dohm-Palmer et al. 2002). As differential rotation acts to destroy substructure through shear, propagation of star formation across significant distances is less likely in such systems. On the other hand, galaxies with solid-body rotation allow for substructure to remain coherent for longer time periods, allowing this mechanism to more efficiently act. The galactic rotation curve for DDO210 from Begum & Chengalur (2004) shows that the central few hundred parsecs of DDO210 are likely undergoing solid-body rotation, further supporting the possibility of migrating star formation in this galaxy. Therefore, assuming these stars formed near where they are presently observed, we conclude the migrating star formation region the most likely explanation for the distribution of Cepheids in DDO210.

7 CONCLUSIONS

Using archival *HST*/ACS imaging of the LG dwarf DDO210, we have detected over 100 pulsating variable stars within this dwarf. These consist of 32 RR Lyrae stars and 75 Cepheids. The properties of these pulsating variables have been compared to the SFH analysis of Cole et al. (2014), showing that the SFH from Cole et al. (2014) is consistent with the properties of the RR Lyrae and Cepheid pulsators. In particular, we find the relatively small population of RR Lyrae stars to corroborate a weak but nonzero star formation rate at ages of ~ 11 Gyr. We find one particularly metal-

poor RR Lyrae that is also consistent with the large spread in the AMR produced by Cole et al. (2014) for these old ages. We find the behavior of the RR Lyrae stars in DDO210 to be consistent with those of other LG dwarfs in the period-amplitude plane. Specifically, this dwarf can be considered an Oo-intermediate system with a striking lack of HASP RRab stars.

As for the Cepheids, we argue that the majority of these stars are short-period CCs, however we cannot rule out the presence of some ACs with the information available to us. We have utilized a period-age relation for CCs in order to estimate the ages of these young pulsators. We find a peak in the Cepheid age distribution near 300 Myr, which agrees well with the SFH from Cole et al. (2014). The youngest of these Cepheids lie offset from the older Cepheids and the centre of the galaxy, confirming previous studies showing the young stars lie offset from the older stars in this galaxy. We conclude that this offset is likely resultant from a migration of star-formation, through a mechanism similar to what was proposed in Dohm-Palmer et al. (2002).

ACKNOWLEDGEMENTS

We thank Karen Kinemuchi for her comments and suggestions on an early draft of this paper that improved its clarity. We are also grateful for the careful reading and helpful suggestions from our referee, Mario Mateo. This work has made use of BaSTI web tools.

REFERENCES

- Alcock, C. et al., 2000, *AJ*, 119, 2194
 Begum, A., Chengalur, J. N., 2004, *A&A*, 413, 525
 Bernard, E. J. et al., 2013, *MNRAS*, 432, 3047
 Brodi, J. P., Madore, B. F., 1980, *MNRAS*, 191, 841
 Bono, G., Marconi, M., Cassisi, S., Caputo, F., Gieren, W., Pietrzynski, G., 2005, *ApJ*, 621, 996
 Cacciari, C., Corwin, T. M., Carney, B. W., 2005, *AJ*, 129, 267
 Catelan, M., Pritzl, B. J., Smith, H. A., 2004, *ApJS*, 154, 633
 Catelan, M., 2009, *Ap&SS*, 320, 261
 Charbonneau, P., 1995, *ApJS*, 101, 309
 Clementini, G., Cignoni, M., Contreras Ramos, R., Federici, L., Ripepi, V., Marconi, M., Tosi, M., Musella, I., 2012, *ApJ*, 756, 108
 Cole, A. A., Weisz, D. R., Dolphin, A. E., Skillman, E. D., McConnachie, A. W., Brooks, A. M., Leaman, R., 2014, *ApJ*, 795, 54
 Coulson, I. M., Caldwell, J. A. R., 1989, *MNRAS*, 240, 285
 Dohm-Palmer, R. C., Skillman, E. D., Mateo, M., et al., 2002, *AJ*, 123, 813
 Dorfi, E. A., Feuchtinger, M. U., 1999, *A&A*, 348, 815
 Fiorentino, G., Limongi, M., Caputo, F., Marconi, M., 2006, *A&A*, 460, 155
 Fiorentino, G., Monelli, M., 2012, *A&A*, 540, 120
 Fiorentino, G., Stetson, P. B., Monelli, M., Bono, G., Bernard, E. J., Pietrinferni, A., 2012, *ApJ*, 759, L12
 Fiorentino, G. et al., 2015, *ApJ*, 798, L12
 Gallart, C., Aparicio, A., Freedman, W. L., Madore, B. F., Martínez-Delgado, D., Stetson, P. B., 2004, *AJ*, 127, 1486
 Glatt, K. et al., 2008, *AJ*, 135, 1106
 Ibata, R. A., Gilmore, G., Irwin, M. B., 1994, *Nature*, 370, 194
 Jacobs, B. A., Rizzi, L., Tully, R. B., Shaya, E. J., Makarov, D. I., Makarova, L., 2009, *AJ*, 138, 332

- Jurcsik, J., Kovács, G., 1996, *A&A*, 312, 111
- Kirby, E. N., Cohen, J. G., Guhathakurta, P., Cheng, L., Bullock, J. S., Gallazzi, A., 2013, *ApJ*, 779, 102
- Klagyivik, P., Szabados, L., Szing, A., Leccia, S., Mowlavi, N., 2013, *MNRAS*, 434, 2418
- Layden, A. C., Ritter, L. A., Welch, D. L., Webb, T. M. A., 1999, *AJ*, 117, 1313
- Lee, Y.-W., Demarque, P., Zinn, R., 1994, *ApJ*, 423, 248
- Mancone, C., Sarajedini, A., 2008, *AJ*, 136, 1913
- Mateo, M., Fischer, P., Krzeminski, W., 1995, *AJ*, 110, 2166
- Mateo, M., 1998, *ARA&A*, 36, 435
- McConnachie, A. W., Irwin, M. J., Ferguson, A. M. N., Ibata, R. A., Lewis, G. F., Tanvir, N., 2005, *MNRAS*, 356, 979
- McConnachie, A. W., Arimoto, N., Irwin, M., Tolstoy, E., 2006, *MNRAS*, 373, 715
- Nemec, J. M. et al., 2013, *ApJ*, 773, 181
- Ordoñez, A. J., Yang, S.-C., Sarajedini, A., 2014, *ApJ*, 786, 147
- Pietrinferni, A., Cassisi, S., Salaris, M., Castelli, F., 2004, *ApJ*, 612, 168
- Pritzl, B. J., Armandroff, T. E., Jacoby, G. H., Da Costa, G. S., 2002, *AJ*, 124, 1464
- Pritzl, B. J., Armandroff, T. E., Jacoby, G. H., Da Costa, G. S., 2004, *AJ*, 127, 318
- Pritzl, B. J., Armandroff, T. E., Jacoby, G. H., Da Costa, G. S., 2005, *AJ*, 129, 2232
- Pritzl, B. J., Venn, K. A., & Irwin, M., 2005, *AJ*, 130, 2140
- Schlafly, E. F., Finkbeiner, D. P., 2011, *ApJ*, 737, 103
- Schroyen, J., De Rijcke, S., Koleva, M. et al., 2013, *MNRAS*, 434, 888
- Searle, L., Zinn, R., 1978, *ApJ*, 225, 357
- Sirianni, M. et al., 2005, *PASP*, 117, 836
- Smith, H. A., 1995, *Cambridge Astrophysics Ser. Vol. 27, RR Lyrae Stars*, Cambridge Univ. Press, Cambridge
- Soszynski, I. et al., 2008, *Acta Astron.*, 58, 163
- Stetson, P. B., 1987, *PASP*, 99, 191
- Stetson, P. B., 1994, *PASP*, 106, 250
- Stetson, P. B., Fiorentino, G., Bono, G., Bernard, E. J., Monelli, M., Iannicola, G., Gallart, C., Ferraro, I., 2014, *PASP*, 126, 616
- Szabados, L., Klagyivik, P., 2012, *A&A*, 537, 81
- Tanvir, N. R., 1997, in *The Extragalactic Distance Scale*, ed. M. Livio, M. Donahue & N. Panagia (Cambridge: Cambridge Univ. Press), 91
- Udalski, A., Szymanski, M., Kubiak, M., Pietrzynski, G., Soszynski, I., Wozniak, P., Zebrun, K., 1999, *Acta Astron.*, 49, 201
- Venn, K. A., Irwin, M., Shetrone, M. D., Tout, C. A., Hill, V., Tolstoy, E., 2004, *AJ*, 128, 1177
- Yang, S.-C., Sarajedini, A., 2012, *MNRAS*, 419, 1362

This paper has been typeset from a $\text{\TeX}/\text{\LaTeX}$ file prepared by the author.